Chapter 4
Phase-Change Materials for Data Storage Applications

Dominic Lencer, Martin Salinga, and Matthias Wuttig

4.1 The Basic Principle of Phase-Change Based Data Storage

A particular promising approach for data storage devices is based on the fast reversible switching of so-called *phase-change materials* between an amorphous and a crystalline state. Both phases are characterized by very different material properties, thus providing the contrast required to distinguish between logical states. Phase-change recording was initiated in the 1960s by S. Ovshinsky [1] and is the state-of-the-art technique for rewritable optical storage. It is also among the most promising candidates to succeed Flash memory as Phase-Change Random Access memory (*PCRAM*) [2–4].

The principle of operation of phase-change based devices is illustrated in Fig. 4.1. A phase-change material is switched between the crystalline and amorphous state by providing a precisely controlled amount of heat. Currently, either laser pulses or electrical pulses are employed as heat sources. Starting from a crystalline bit, the temperature needs to be elevated above the liquidus temperature T_l using a short, high intensity (high current) pulse. Since only a spatially confined region is heated up, a huge temperature gradient between the molten bit and the surrounding material is obtained, leading to high cooling rates of about 10^{10} K/s once the external stimulus is turned off. If the melt cools fast enough, crystallization is bypassed and a melt-quenched amorphous bit is formed once the temperature falls below a critical temperature, the glass transition temperature T_g. In this temperature regime, the

D. Lencer • M. Salinga
I. Physikalisches Institut (IA), RWTH Aachen University, 52056 Aachen, Germany

M. Wuttig (✉)
I. Physikalisches Institut (IA), RWTH Aachen University, 52056 Aachen, Germany

JARA-FIT, I. Physikalisches Institut (IA), RWTH Aachen University,
52056 Aachen, Germany
e-mail: wuttig@physik.rwth-aachen.de

S. Hong et al. (eds.), *Emerging Non-Volatile Memories*,
DOI 10.1007/978-1-4899-7537-9_4

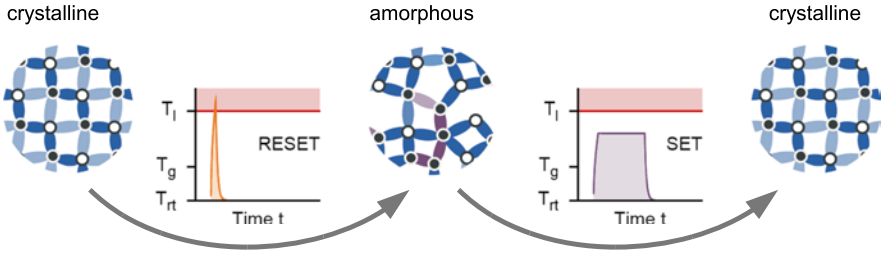

Fig. 4.1 The operation principle of phase-change devices is based on the reversible switching between the crystalline and amorphous state. Amorphization (also called *RESET*-operation) of a bit proceeds via melt-quenching, employing short current or laser pulses as heat sources. Here, a huge temperature difference between the confined melt and the surrounding material leads to extremely high cooling rates. Thus, the disorder of the liquid is frozen in. Crystallization (*SET-operation*) requires annealing of an amorphous bit at a temperature below the melting temperature for the atoms to adopt the energetically favorable crystalline order. From [5]

atomic mobility is so small that crystallization, though energetically favorable, is kinetically hindered. To switch from the amorphous back to the crystalline state, the temperature of the bit needs to be elevated for a sufficiently long period of time to a temperature where the atomic mobilities are high enough for crystallization to occur. Hence, the sample has to be heated significantly above the glass transition temperature. To read out whether a bit is amorphous or crystalline, low intensity (low current) pulses are employed to distinguish between low and high reflectivity (conductivity). Noteworthy are the timescales of phase-change recording; crystallization is typically the slowest process involved. Nevertheless, under optimal conditions it may proceed in a matter of nanoseconds. At ambient conditions, however, crystallization of an amorphous bit must not take place within many years to ensure data retention. This means that the crystallization rate of phase-change materials must increase by up to twenty orders of magnitude while the temperature is elevated by only a few hundred Kelvin. Besides the phase transition kinetics, optical and/or electrical contrast is of utmost importance for phase-change materials. In order to distinguish between the phases, their material properties, namely resistivity and conductivity, must differ significantly. In addition, specific applications call for further requirements, such as a small density change upon crystallization.

A number of materials have empirically been confirmed to meet the requirements named above. Most of the material families already identified can be found in the ternary Ge:Sb:Te-phase diagram shown in Fig. 4.2. On the pseudo-binary line connecting GeTe and Sb_2Te_3, the most prominent materials such as $Ge_2Sb_2Te_5$ are located [6, 7]. Besides Sb_2Te_3, also Sb_2Te offers suitable properties when combined with fractions of silver and indium, for instance, yielding the widely employed AgInSbTe (abbrev. AIST) [8]. Finally, another material family that has attracted considerable interest in the last years is found here, namely modifications of antimony such as $Ge_{15}Sb_{85}$ [9, 10]. It stands out since it does not contain a chalcogen

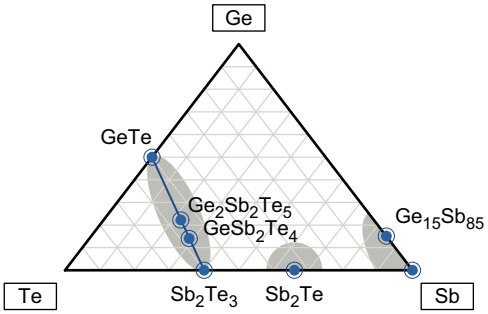

Fig. 4.2 Most phase-change materials are found within the ternary Ge:Sb:Te-phase diagram. In particular, the pseudo-binary line between GeTe and Sb_2Te_3 stands out as it hosts the most prominent phase-change materials composed as $(GeTe)_m(Sb_2Te_3)_n$, with m and n being integer numbers. From [5]

component, despite the fact that this was commonly assumed to be a requirement. It can be understood as "doped" antimony.[1]

For the development of phase-change materials, it is necessary to understand the phases involved in phase-change recording, that is liquid, amorphous, and crystalline phase. This is a challenging task since none of the employed phases represents equilibrium-conditions, either inherently (amorphous phase) or due to the fast switching. Thus, since the phases are not unique (i.e., depending on the preparation conditions), their characterization is hampered. Furthermore, also the transition between the phases needs to be investigated and modeled. It is the aim of this chapter to briefly review the current state of research on selected aspects of phase-change materials. Therefore, one switching cycle, that is from crystalline over the liquid to the amorphous state, and back again to the crystalline state, is discussed.

4.2 The Crystalline Phase

The crystalline structures of phase-change materials, such as the well-studied and widely employed Ge:Sb:Te-materials (e.g., $Ge_2Sb_2Te_5$), typically exhibit a number of generic features. Along the lines of Da Silva et al. [11, and the references therein], the two limiting cases of the pseudobinary line, GeTe and Sb_2Te_3, are well suited to discuss these. GeTe exhibits a structure that closely resembles the rocksalt-structure, with Ge occupying the cation, and Te the anion sublattice. Yet, at temperatures below approximately 700 K, there is a displacement of the atomic positions along the [1 1 1]-direction. This leads to a splitting of the bonds from six equal to three strengthened, short and three weakened, long ones. These Peierls-like distortions

[1] Doping in the field of phase-change materials refers to much larger concentrations (typically on the order of some percent) than in usual semiconductors.

lead to an opening of the gap, and reduce the energy of the occupied states. The unit cell exhibits a slight rhombohedral distortion as a consequence of the atomic displacement [see 12, and references therein]. Also the structure of Sb_2Te_3 can be understood in terms of a distorted rocksalt-like atomic arrangement. Again, there is an atomic alternation, and antimony has only tellurium neighbors in an octahedral environment. Yet, the sequence of alternating layers ("Te–Sb–Te–Sb–Te") is terminated by adjacent Te-planes due to the tellurium-excess. The distance between these Te-planes is large compared to the Sb–Te-distances, and the bonding between them is explained in terms of the Van der Waals-interaction.

The Ge:Sb:Te-compounds inherit the structure ingredients mentioned before. In the metastable crystalline phase formed by fast annealing, they exhibit a rocksalt-like structure, with tellurium occupying the anion sublattice. The cation sublattice is initially randomly occupied by germanium, antimony and intrinsic vacancies. Thus, there is atomic alternation and a principal octahedral coordination. Via density functional theory calculations, energetically optimal sublattice occupations, towards which the systems tend by annealing, have been determined [11, 13, 14]. Yet, the theoretically most favorable structure is likely not obtained in experiments given the mismatch between optical properties calculated for those structures and measured ones [15]. Just like, GeTe, the atomic positions exhibit (Peierls-like) distortions from the high-symmetry-positions. The magnitude of the atomic displacements has been determined to amount to about 0.2 Å per atom by a variety of experimental [16, 17] and theoretical investigations [18–21]. For compositions close to GeTe, also a rhombohedral distortion of the unit cell is observed [22]. The aforementioned occurrence of intrinsic vacancies in the Ge:Sb:Te-systems, a rather unusual structural feature, has attracted considerable interest [23]. It has been argued to arise to balance the number of p-electrons per lattice site, $N_p{}^{\square}$. The respective count given n_i atoms per formula unit reads

$$N_p^{\square} = \frac{2n_{Ge} + 3n_{Sb} + 4n_{Te}}{n_{Ge} + n_{Sb} + n_{Te} + n_V}. \tag{4.1}$$

Those compositions along the GeTe–Sb_2Te_3 pseudobinary line that form stable phases correspond to a number of three with $n_V = n_{Te} - (n_{Ge} + n_{Sb})$ (i.e., by balancing the mismatch between the number of anions and cations by intrinsic vacancies).

The atomic arrangement and the resulting electronic structure of phase-change materials in the crystalline phase have been identified as key to understanding the contrast between the phases. Investigations of the dielectric function at and below the band gap have shown that phase-change materials exhibit a significant increase of the low-energy limit of the real part of the dielectric function (i.e., ε_∞) in the crystalline phase that is absent in both the amorphous phase and other semiconductors [24]. This electronic polarizability enhancement stems from a peculiar type of covalent bonding called *resonant bonding*; in a situation where more bonds are formed than can be saturated with the present number of valence electrons—the ratio being about two for phase-change materials—the groundstate wavefunction can be viewed as a superposition of energetically equivalent *contributing states* in

which only saturated bond are allowed. The energy of the system is reduced as compared to the energy of the contributing states by the resonance energy. Depending on the amplitude of the resonance energy, the electronic structure is very sensitive to external perturbations. This leads to the fingerprint effects of resonant bonding, large optical dielectric constants ε_∞, and Born effective charges $Z*$ [25]. The resonance is counteracted by the static, Peierls-like atomic distortions that lead to a smaller number of more saturated covalent bonds. Nevertheless, for small distortions resonance effects are weakened but prevail; density functional perturbation theory calculations on GeTe prove, that, while the Peierls-like distortion and the subsequent cell distortion significantly reduce the values of Born effective charge and optical dielectric tensor, they nevertheless remain anomalously large [12].

In order to assist this design rule, it is desirable to have a simple recipe for suitable materials. Based on the work by Littlewood [26], a two-dimensional map has been proposed [12], see Fig. 4.3. It is spanned by two coordinates, r'_σ and r_π^{-1}, that provide measures of the ionicity of the bonding and the tendency towards hybridization, respectively. The former quantity is derived from the size mismatch of the constituting atoms, the latter from the energetic splitting of s- and p-levels; the

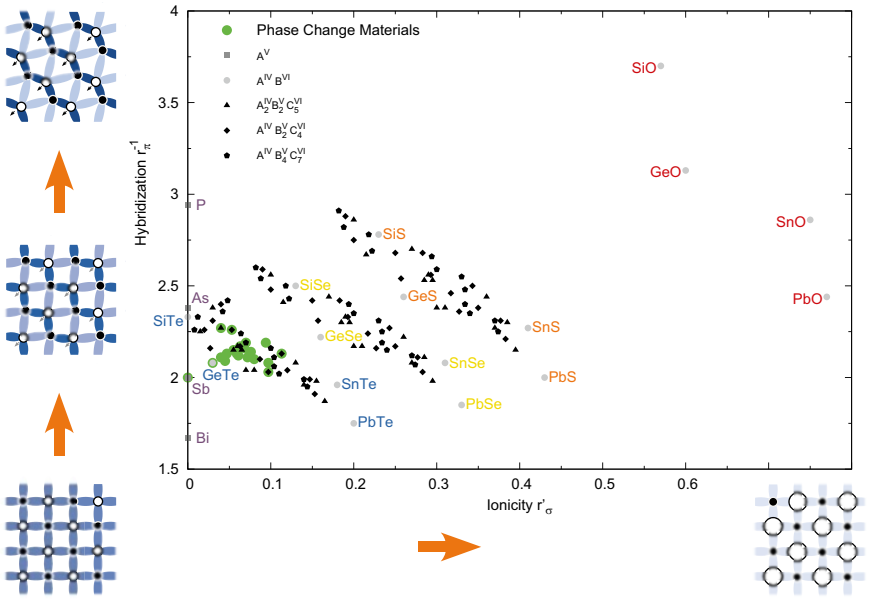

Fig. 4.3 Empiric map for materials with about three p-electrons per atomic site and even numbers of anions and cations. The axes that span the map are the tendency towards hybridization, r_π^{-1}, and the ionicity, r_σ', both defined in the text. The coordinates of a large number of materials have been calculated (see the supplement to [12] for an index of materials). Phase-change materials are located within a small region of the map that is prone to the occurrence of resonant bonding. The graphs on the outside illustrate the weakening of resonance effects as one leaves this region due to the formation of less, more saturated covalent bonds via distortions or due to charge localization at the ions due to increasing ionicity. From [12]

larger the split, the less likely is hybridization, which is required for atomic distortions. A pronounced ionicity is unfavorable for phase-change materials since it weakens the covalent (resonant) bonds. A significant probability of hybridization/atomic distortions, on the other hand, also counteracts the resonance-character of the bonds. Thereby, phase-change materials should be located in a region of the map where both quantities are small to ensure the required contrast. Indeed, empirically identified phase-change materials shown as green dots in Fig. 4.3 span only a small region in the lower left corner.

The electrical properties of crystalline phase-change materials are dominated by the tendency towards forming large quantities of defects. As has been shown for GeTe [27], this shifts the Fermi-energy into the valence band, giving rise to p-type conductivity. Hence, the conductivity in the crystalline phase typically is metal-like, and orders of magnitudes larger than in the amorphous phase [28, 29]. Recently, it has been shown that disorder, likely due to the sublattice occupation, has a pronounced impact on the electronic mobility. In result, a metal-insulator-transition is observed for multi-component materials such as $GeSb_2Te_4$ upon annealing, by which ordering of the sublattice is thermally triggered [30].

4.3 From the Crystalline to the Amorphous Phase

After a basic introduction into the phase-change cycle has been given already in the beginning of this chapter, a more detailed view shall be presented here. Therefore, Fig. 4.4 shows the phase transitions in terms of a time–temperature-transformation diagram. As this figure describes, the principle of phase-change materials relies on a peculiar interplay of the temperature-dependent atomic mobility D, that is inversely related to the macroscopic viscosity η via the Stokes–Einstein relation,

$$D(T) \propto T / \eta(T) \tag{4.2}$$

and Gibbs free energy G. The difference in G between the phases is the driving force for phase transitions; in equilibrium, the phase that minimizes G is adopted, but on small timescales, the finite atomic mobility kinetically hinders the establishment of equilibrium conditions. This enables the preparation of glassy bits by "freezing" a configuration of the undercooled liquid.

4.3.1 Glass Formation

As a melt is quenched, it becomes increasingly rigid. Once a critical temperature, the glass transition temperature T_g, is passed and given that crystallization has been avoided, the atomic mobility becomes too small for structural rearrangements as required to reach equilibrium. Small atomic mobilities at ambient temperatures are

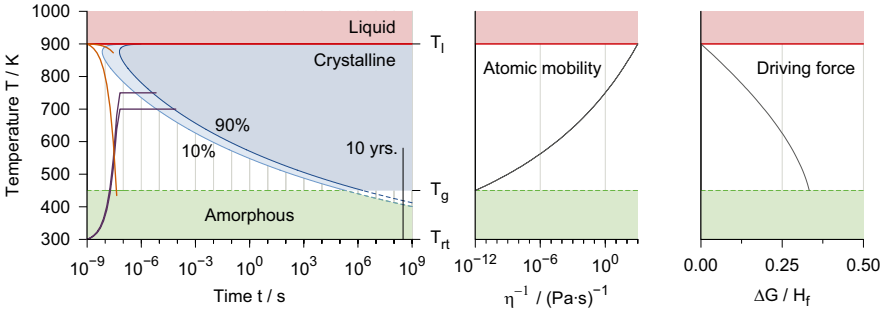

Fig. 4.4 The graph on the *left* schematically shows the transformation of a fixed volume of a phase-change material depending on the time spent at a certain temperature. The crystallization of 10 and 90 %, respectively, of the material is indicated by *grey lines/areas*. As one cools the melt below the liquidus temperature T_l (typically around 900 K), the atomic mobility, shown in the *middle*, is very large. However, since the driving force for crystallization, that is the difference in Gibbs free energy between (undercooled) liquid and crystal, visualized on the right in units of the heat of fusion H_f, is small, crystallization does not take place immediately. It may thus be bypassed, if the melt is quenched sufficiently fast. This is visualized by two constant rate-quenching processes starting at T_l, the slower of which leads to partial crystallization. Typically, quenching rates of 10^{10} K/s are required. At low temperatures, the driving force becomes larger, but the vanishing atomic mobility kinetically hinders crystallization. Eventually, as the glass transition temperature T_g (typically ranging around half T_l) is passed, an amorphous bit is formed. While ideally it is long-time stable against crystallization at ambient conditions, it crystallizes in fractions of seconds if the temperature is elevated and kept for a sufficiently long time. Two annealing processes starting at room temperature T_{rt} are indicated. Obviously, crystallization time and temperature are mutually dependent. From [5]

a key requirement for the stability of an amorphous bit. The mobilities, on the contrary, must not be small at elevated temperatures to enable fast crystallization. The glass transition temperature is commonly defined as the temperature, at which the viscosity equals $1 \cdot 10^{12}$ Pa s. The resulting glass is out of thermal equilibrium. Thus, a glass is always subject to "aging" effects, evidencing the relaxation towards equilibrium conditions.

To assess the ease of glass formation, it is instructive to note that the shape of the area in Fig. 4.4 that refers to crystallization is strongly affected by the temperature-dependence of the viscosity. Whether a glass may be formed at small cooling rates (*easy glass former*) or whether this may only be facilitated via rapid quenching (*marginal* or *bad glass former*) as in the case of phase-change materials, can thus be linked to the viscosity. The temperature-dependence of η varies among materials as is shown in Fig. 4.5. If it is Arrhenius-like, a liquid is called *strong*. However, many materials exhibit a behavior empirically described by the Tamann–Vogel–Fulcher ansatz

$$\eta(T) = \eta_0 \cdot \exp(A / (T - T_0)) \tag{4.3}$$

with η_0, A and T_0 being constants. Such liquids are referred to as *fragile*. As a measure of the deviation from Arrhenius-behavior, the fragility m is introduced as a steepness-index at T_g via

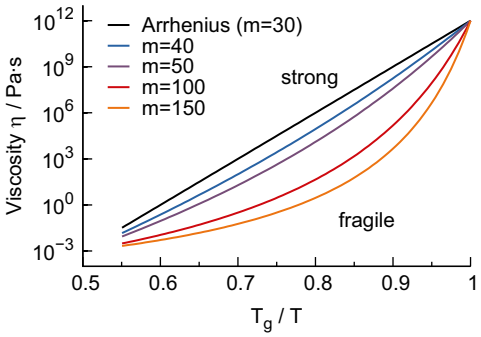

Fig. 4.5 The viscosity of a liquid typically depends exponentially on temperature. If the dependence is Arrhenius-like, it is called a strong liquid. If the dependence at T_g is steeper, the liquid is referred to as fragile. The deviation from Arrhenius-behavior is indicated by the steepness at T_g, the fragility m. From [5]

$$m = \frac{\partial(\log_{10}\eta)}{\partial(T_g / T)} \,|\, T = T_g \,. \tag{4.4}$$

A detailed review of these aspects has been given by Angell et al. [31]. For phase-change applications, a rather fragile liquid appears favorable since the crystallization speed would increase with temperature (above T_g) more rapidly.

Glass transition temperatures can experimentally be assessed via differential scanning calorimetry since the transition from the glass to an undercooled liquid appears as an endothermic step. Such measurements have shown that for phase-change materials, T_g adopts values of about 450 K, ranging around half the liquidus temperatures [32]. Empirically, this ratio between T_g and T_l characterizes phase-change materials as marginal glass formers [see 33, and the references therein].

4.3.2 Glass Rigidity and Bond Constraint Theory

In order to design a phase-change material, it is desirable to have a theory that connects stoichiometry with structure, but also with glass forming ability. Thus, the concept of *bond constraint theory* will be briefly explained. This theory is an approach to characterize the rigidity of an amorphous covalent network, based on the (mean) atomic coordination. In order to fix an object at a given place, three constraints are required. If more are present, the loss of one does not generally lead to the release of this fixation. Less constraints, on the other hand, leave open degrees of freedom, giving room to limited movement (i.e., so-called floppy modes). It is hence reasonable to classify covalent networks such as glasses according to the number of constraints per atom, n_c. An *ideal* glass has a value of three, whereas *floppy* glasses have less and *stressed rigid* glasses more constraints per atom.

Moreover, bond constraint theory also provides a link between n_c and the experimentally accessible coordination number, r. Given that in a covalent network the number of bond-stretching constraints equals half the number of bonds and the respective number of bond-bending constraints sums up to $2r - 3$, then the total relationship as proposed by Phillips [34] reads

$$n_c(r) = \frac{5}{2}r - 3 \Leftrightarrow r = \frac{2}{5}(n_c + 3). \tag{4.5}$$

This implies that in an ideal glass, $n_c = 3$, the average coordination should take the value 2.4. Vice versa, since the average coordination is often characteristic for an atomic species, changing the stoichiometry of a glass allows to modify r and thereby to affect the rigidity of the glass. In this context, it is worth noting the so-called $8 - N$-rule; with N being the number of valence electrons of an atom, this rule states that generally, the coordination in a covalent environment is equal to $8 - N$. For instance, germanium with its two s- and two p-valence electrons is expected to be fourfold coordinated, while antimony would accordingly adopt a threefold and tellurium a twofold coordination. The $8 - N$-rule successfully explains and predicts the atomic coordination for a wide range of materials composed of elements from the groups V, VI, and VII [35]. But as one goes down in the fourth column of the periodic table, the limits of the $8 - N$-rule become obvious; elemental lead is not tetrahedrally, but octahedrally coordinated, owing to the fact that due to relativistic effects hybridization becomes unfavorable [26].

It has been found that in many cases it is not a single point but rather an extended region, the so-called intermediate phase, which separates floppy and stressed rigid glasses. Thus, instead of one there are two rigidity transitions upon variation of r as evidenced by experiments for chalcogenide glasses, with the intermediate phase marking a range of *isostatic* rigidity [36]. Interestingly, a link between rigidity of the glass and the temperature-dependence of the viscosity of the liquid has been discussed. In [37], it has been claimed that both floppy and stressed rigid glasses exhibit fragile liquids, whereas intermediate glasses should exhibit strong liquids.

Easy glass formation is expected only for ideal/intermediate glasses [37]. This is unfavorable for fast crystallizing phase-change materials as argued before. Indeed, typical phase-change materials yield, according to the $8 - N$-rule, numbers of r between 2.6 and 3.2, locating them in the region of stressed rigid glasses. The coordination numbers derived from structural investigations (see Sect. 4.4.1) tend to be higher as will be shown below, so phase-change materials are seemingly even more stressed rigid than expected by the $8 - N$-rule. Recently, extensive work on the rigidity and application of bond constraint theory in the ternary Ge:Sb:Te phase diagram has been presented by Micoulaut et al. [38]. Employing density functional theory calculations, these authors were able to prove that phase-change materials indeed fall into the stressed rigid regime.

Due to the importance of T_g for data retention, a large body of work on phase-change materials is concerned with means of material modifications to increase the value of T_g. In general, a host phase-change material such as $Ge_2Sb_2Te_5$ or antimony

is chosen for its optical and electrical properties in the amorphous and crystalline phase. Then, the impact of the addition of other elements is investigated. In the framework of bond constraint theory, the observed increase of T_g via the addition of so-called network forming elements, for instance from group IV, to a host phase-change material can be understood by the resulting increase of the average coordination number r. One important aspect not included in bond constraint theory, though, is the fact that not only the number of bonds but also the bond energies need to be taken into consideration. Thus, the dependence of T_g on r via stoichiometry variation may deviate from a monotonous increase. An improved model was proposed by Lankhorst [39] (see also [40]) that empirically relates T_g to the enthalpy of atomization of an amorphous network. The latter is calculated from the bond enthalpies of all bonds present in the system. It has been successfully applied to resolve the impact of Al- and Cu-doping on the glass transition temperature in Ge:Sb and Sb:Te as has been confirmed by experiment [41]. A complimentary study on Al-doping of Ge:Te was conducted by Katsuyama and Matsumara [42]. The Lankhorst-model comes at the expense of simplicity as for the bond energies the atoms participating in each bond need to be explicitly known. Hence, structural information on phase-change materials in the amorphous phase is required.

4.4 The Amorphous Phase

The amorphous phase of typical phase-change materials is studied intensively regarding two aspects; the structure is investigated in order to link it to the properties of the glass as well as the fast kinetics. Its electrical conductivity, on the other hand, is of crucial importance for upcoming electrical memories. Both fields shall be addressed in this section.

4.4.1 Atomic Structure

Since amorphization via melt-quenching relies on a rapid decrease of atomic mobilities, it can be expected that the glass inherits structural features of the liquid. Consequently, the investigation of the structure of both the liquid and the amorphous phase is of interest. The aim of these studies is twofold; on the one hand, similarities and differences with respect to the crystalline phase are investigated. This way, the contrast between the phases could possibly be linked to the difference in bonding. Moreover, it is often argued that fast kinetics would imply that the structural rearrangements upon crystallization are necessarily small. On the other hand, the identification of coordination numbers and bond types enables the application of concepts introduced in the last section, such as bond constraint theory, beyond approximations (e.g., without relying on the $8 - N$-rule).

As of today, there are numerous experimental and theoretical studies available in the literature. Regarding the liquid phase, Steimer et al. [43] performed neutron diffraction experiments on a wide range of materials, and found that phase-change materials exhibited octahedral coordination. Further confirmation of the prevalence of this structural motif is given by theoretical studies [44]. Moreover, an alternation between atomic species (e.g., ABAB) is observed [20]. Thus, the structure of the melt is apparently similar to that of the crystalline state. The identification of octahedral or tetrahedral bonding geometries is a recurring motif in the literature. The reason why the occurrence of octahedral geometries is of interest is the fact that it is rather unexpected according to the $8 - N$-rule. For germanium, sp_3-hybridization may be regarded as the energetically most favorable electronic structure to achieve a fourfold coordination as adopted in elemental germanium. The presence of non-tetrahedrally coordinated germanium in phase-change materials thus is remarkable and clearly caused by its bonding environment.

The vitrified, amorphous phase is easier to investigate as the temperature does not need to be elevated. Yet, the published studies, that treat GeTe and $Ge_2Sb_2Te_5$ in particular, come to significantly different conclusions. The problem, to what extent the experimental results depend on the sample preparation and thermal history, remains unclear as of this writing. In many studies, the use of as-deposited amorphous samples is necessary to yield the required, large amount of amorphous material. Yet, the kinetics of as-deposited amorphous and melt-quenched amorphous phase differ significantly, which must have its origin in structural differences [45].

Initially, EXAFS- and XANES-data (extended x-ray absorption fine structure and x-ray absorption near-edge spectroscopy, respectively) were interpreted in terms of the so-called umbrella flip-model, where germanium switches from tetrahedral to octahedral positions upon crystallization. Apart from this, chemical ordering and octahedral bonding of the remaining species was concluded [16, 46]. Many successive studies interpreted the phase transition along the lines of this model, see, for instance, [47–50]. Subsequent experimental studies, in particular those by Jovari et al. [51, 52], rejected such simple structural models, yet confirmed the presence of tetrahedral coordination of germanium. Kohara et al. [53], on the contrary, found a correlation between tetrahedral coordination and the occurrence of homopolar bonds; due to chemical ordering in $Ge_2Sb_2Te_5$ and thereby the absence of homopolar (or Ge–Sb) bonds, octahedral coordination was obtained for germanium.

The obvious differences between structure models derived from experiments alone have motivated various large-scale molecular-dynamics simulations. Materials investigated span the pseudobinary line $(GeTe)_m(Sb_2Te_3)_n$ from GeTe [54, 55] over $Ge_8Sb_2Te_{11}$ [56] and $Ge_2Sb_2Te_5$ [20, 21, 54, 57–60] to Sb_2Te_3 [61]. In these simulations, the link between tetrahedral germanium and the occurrence of bonds other than Ge–Te is confirmed. The concentration of tetrahedral germanium is about one third, leaving octahedrally coordinated germanium atoms as the majority species. Moreover, cavities as precursors of the intrinsic vacancies found in the metastable crystalline phase have been identified. It is observed that coordination numbers—despite the ambiguity in defining them—tend to be slightly larger than those derived

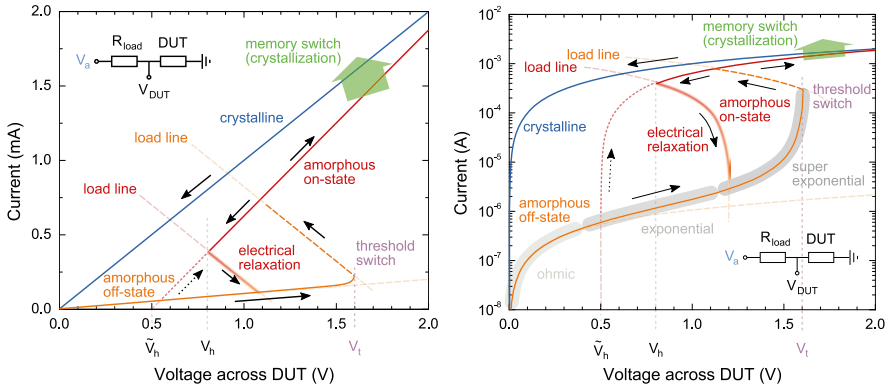

Fig. 4.6 The current–voltage characteristics of phase-change materials (device under test, DUT), shown schematically in both linear (*left*) and logarithmic scaling (*right*), exhibit an interesting effect called threshold switching. For small electric fields the curves of the low resistive, crystalline and the high resistive, amorphous phase differ significantly. However, the situation changes if a critical voltage (corresponding to a field strength of some ten V/μm) is exceeded. The amorphous phase suddenly becomes much more conductive, switching to the so-called *ON-state* as opposed to the *OFF-state*. This effect, called threshold switching, enables sufficient joule heating for crystallization (memory switching) at moderate voltages. Further aspects of threshold switching marked in the graphs are discussed in the text. From [65]

from the 8 – *N*-rule. Hence, phase-change materials are seemingly even more stressed rigid than expected from the 8 – *N*-rule.

4.4.2 *Electrical Properties*

The electrical conductivity of amorphous phase-change materials exhibits a pronounced dependence on the strength of the applied electric field as shown in Fig. 4.6. Two states can be discerned, the amorphous *OFF*- and *ON*-states. Until a critical field is reached, the threshold field E_t (or threshold voltage V_t), the system remains in the OFF-state. Here, the conductivity remains small and exhibits a thermally activated transport behavior,

$$\sigma(T) = \sigma_0 \exp(-\overset{\text{A}}{E}_{\text{cond.}} / kT) \tag{4.6}$$

with an activation energy of approximately half the measured optical gap, $E_A^{\text{cond.}} \approx 1/2 E_G^{\text{opt}}$. When the field exceeds the threshold value, the conductivity increases significantly (ON-state). Threshold fields are typically about some ten V/μm ([62] and the references therein [63, 64]). From a technical point of view, this behavior is very desirable since crystallization of an amorphous bit is facilitated via Joule-heating. Without the *threshold switching*, large voltages would need

to be applied in order to drive a sufficiently large current for heating and thus crystallization to occur. Threshold switching is to be distinguished from *memory switching* that refers to crystallization, whereas threshold switching is a fully reversible phenomenon specific to the amorphous phase.

The discovery of threshold switching for data storage devices dates back to the pioneering work by Ovshinsky [1], and many models have been proposed to account for it ever since. Most authors suppose that threshold switching is an electronic (rather than a thermal or structural) effect. Emin [66] concludes that at elevated fields, the density of small polarons becomes larger. Thus, due to their proximity, lattice deformation becomes unfeasible once the threshold field is reached. Therefore, carriers may not localize anymore and the material becomes highly conductive. In the picture of Ielmini and Zhang [67], Ielmini [68] (and the references therein), that is Poole–Frenkel conduction, the electric field increases the probability of a carrier that occupies one trap to get to another one nearby. At low fields, this requires extended states. At the threshold field, also direct tunneling becomes possible, leading to the conductivity increase. Another model presumes that threshold switching stems from a field- and carrier density-dependent generation mechanism, thus providing a positive feedback once a critical field is attained. At low fields, however, recombination counterbalances the generation [62, 69, 70]. There are various possible microscopic models that could account for this phenomenological effect such as impact ionization [71]. An alternative to the electronic models of threshold switching is provided by field-induced nucleation [72]. It is argued that at the threshold field, a crystalline filament forms in the amorphous volume, connecting the electrodes. The origin of this effect is ascribed to a field-dependence of the free energy of the system. For further details, the interested reader is referred to [4, 65].

An issue important for so-called *multi-level storage* is the drift of the amorphous resistivity with time. Multi-level storage aims at increasing the storage density by differentiating more than two logical states per cell. This is done by varying the volume of the amorphized part of the cell. However, one finds that the resistivity of a (partially) amorphous cell steadily increases with time. Multi-level storage is only feasible, if this drift is confined to a small resistivity interval associated with one logical state. The increase obeys a power law dependence on time. As the process is temperature-activated, it can be accelerated by raising the temperature. Since progressing crystallization is expected to lead to a drop in resistivity as the crystalline phase is more conductive, drift cannot be explained by the formation of crystalline nuclei. Moreover, since also threshold voltages tend to drift in the same fashion, a common origin of both effects is anticipated. There are multiple candidates to explain the resistance drift effect. Yet, this topic is still up to debate. Most authors consider a general time and temperature-dependence of the parameters entering Eq. (4.6), in particular of the activation energy [73].

On the one hand, a change in the size of the gap due to stress relief has been discussed. In this universal model, hydrostatic pressure is exerted on the amorphous volume after quenching due to the significant density increase as seen by X-ray reflectometry measurements [74]. The stress causes the gap and thus the activation energy to decrease. The recovery of the gap then leads to the observed drift [75, 76].

On the other hand, models involving a change in the occurrence of particular electronic states have been proposed. More specifically, the presence of valence alternation pairs (VAPs) and an increase in their number, resulting in an increasing resistivity, have been suggested [75, 77]. This, however, is to be contrasted with studies that question the presence of VAPs in phase-change materials [21, 78]. Another model (see [79] and references therein) also aims at localized states at the gap edges, which might arise as tails; charge transport via hopping involving these states is hampered, if the respective density of states decreases. If the states vanish due to structural relaxation, a decrease in the hopping-conductivity results in a resistance drift. In addition, the position of the Fermi-level may be expected to move towards the middle of the gap, if it had previously been pulled towards one edge by these states.

4.5 Crystallization of an Amorphous Bit

After the discussion of the properties of both the crystalline and the amorphous phase, as well as the process of amorphization in the preceding sections, only the process of crystallization remains to return to the initial point of the phase-change cycle. Commonly, this phase transition is modeled along the lines of the classical theory of crystallization.

4.5.1 Classical Theory of Crystallization

Within this theoretical framework, two mechanisms of crystallization are discernible, nucleation and growth. Nucleation is the process of forming a crystalline nucleus within an amorphous matrix. Growths refers to the progression of the phase front separating amorphous and crystalline regions. The driving force for crystallization is the free energy gain. Since an energy barrier separates amorphous and crystalline structures, sufficient thermal energy has to be provided to enable the system to overcome it. Nucleation is typically modeled in a continuum-approximation, neglecting the discrete atomic structure. Then, the formation of a crystalline nucleus involves the formation of a continuous interface. The difference in free energy $\Delta G(r)$ for a spherical crystalline cluster of radius r within a liquid (undercooled melt) is

$$\begin{aligned}\Delta G(r) &= V(r)\cdot\Delta G_V + A(r)\cdot\sigma \\ &= \frac{4}{3}\pi r^3\cdot\Delta G_V + 4\pi r^2\cdot\sigma\,,\end{aligned} \tag{4.7}$$

with V and A being volume, and surface of the nucleus, ΔG_V the difference in G between the two phases per unit volume, and σ the interfacial energy per unit surface area. At the critical radius,

$$r_c = \frac{2\sigma}{|\Delta G_V|} \tag{4.8}$$

$\Delta G(r)$ exhibits a maximum. So only nuclei of a sufficient initial size larger than r_c gain energy by growth. Below this critical size, their dissolution is energetically preferred as it removes the interface. According to Becker and Döring, a steady-state distribution of subcritical clusters is formed after an incubation time τ. Recently, Lee et al. [80] proposed fluctuation transmission electron microscopy to experimentally study the evolution of such subcritical nuclei in thin films upon laser irradiation. From the steady-state distribution, a steady-state nucleation rate I_{ss} given by

$$I_{ss} \propto \eta(T)^{-1} \exp\left(-\frac{\Delta G(r_c)}{k_B T}\right) = \eta(T)^{-1} \exp\left(-\frac{16\pi}{3k_B T}\frac{\sigma^3}{(\Delta G_V)^2}\cdot f(\theta)\right) \tag{4.9}$$

is derived. For the moment, we shall neglect the factor $f(\theta)$, thus setting it to unity. Once postcritical crystalline nuclei have been formed, their speed of growth for sizes $r \gg r_c$ is derived in the framework of classical crystallization theory as

$$u(T) = \frac{\partial r}{\partial t} \propto \frac{T}{\eta(T)}\left[1 - \exp\left(-\frac{\Delta G(T)}{k_B T}\right)\right]. \tag{4.10}$$

The temperatures at which nucleation and growth exhibit their respective peak values are not the same. Furthermore, process might be more dominant than the other. Hence, nucleation-dominated and growth-dominated crystallization have been observed in the rather large volumes encountered in optical recording, leading to a sub-classification of phase-change materials. In the case of nucleation-dominated crystallization, the time it takes to crystallize an amorphous bit does not depend on its volume to a first approximation. Growth-dominated materials, on the contrary, do exhibit a volume dependence; the smaller the volume, the quicker it is completely crystallized [81]. In general, the sub-classification becomes less helpful for small volumes, where geometry and interfaces play a more important role, increasing the contribution of crystal growth to the transformation. By amorphization of a bit, usually a crystalline rim is created. Hence, the process of growth is typically decisive in electronic phase-change memories, also because no incubation time as for nucleation is involved.

So far, we have only considered homogeneous phases. However, the activation energies can be affected by introducing heterogeneities. This is incorporated into the framework of crystallization theory by the factor $f(\theta)$, with θ being the wetting angle. Impurities and interfaces can catalyze nucleation, but also, they can hinder growth. If heterogeneous sites play a dominant role, crystallization shifts from being triggered in the whole volume of the material to the vicinity of these heterogeneous sites. Interfaces are almost inevitable in phase-change recording. In nanoscaled electrical devices, their presence near the active material cannot be avoided.

In fact, the choice of the dielectric capping material in optical discs [82, 83] or electrode material in electrical memory cells [84] has been shown to significantly influence the crystallization behavior; below a thickness of about 5 nm, crystallization temperatures are even dominated by the choice of the interface material.

The actual configuration of the amorphous phase itself has a pronounced impact on the crystallization properties. Particular structural features of an as-deposited amorphous phase, that are not present in a melt-quenched amorphous phase, might vanish for good after the first crystallization, and thus be irrelevant for applications that involve countless numbers of cycles. Various authors have noted that the first crystallization of an as-deposited amorphous phase may be different from recrystallization of a melt-quenched phase [85–88].

As mentioned already in Sect. 4.3.2, tuning the crystallization kinetics by "doping" (stoichiometry variation) is routinely investigated in the field of phase-change materials. The interested reader is referred to the article of Zhou [89]. Notably, two scenarios can be discerned; a nucleation-dominated material may crystallize faster if doped with a certain element. However, the same dopant may impede growth in a growth-dominated material.

One can distinguish between three temperature regimes relevant for research on the crystallization kinetics. The first regime is located at around the glass transition temperature. In this temperature interval, crystallization ought to proceed very slowly. Experimentally, this enables the direct observation of nucleation and growth. This has been demonstrated using high-resolution transmission electron microscopy [90, 91] and atomic force microscopy [92]. From such measurements, data retention at a given temperature can be assessed. A second temperature regime of interest is situated at around the liquidus temperature. The small driving force for crystallization enables to study the undercooling of droplets employing differential thermal analysis, and thereby the determination of the interfacial energy σ [93]. The experimentally most challenging yet technologically relevant temperature regime is located in the temperature regime where crystallization proceeds the fastest. Here, materials are tested under operation conditions, either embedded in production-type samples or using specialized equipment to spatially and or temporally resolve the phase transition. In particular, the minimum crystallization time is assessed this way.

Information on the physical processes that lead to crystallization can also be reconstructed from the morphology of a crystallized bit [85, 94, 95]. In particular transmission electron microscopy as presented by Friedrich et al. [96]—shown in Fig. 4.7—yields detailed insight into the distribution and shape of crystallites, from which the distribution of nuclei and their growth may be inferred.

4.5.2 Atomistic Modeling of Crystallization

So far, we have employed the continuum approximation, neglecting the discrete atomic structure. The energy barrier separating the phases has not been linked to the composition or the microscopic structure. Thus, it is desirable to improve the

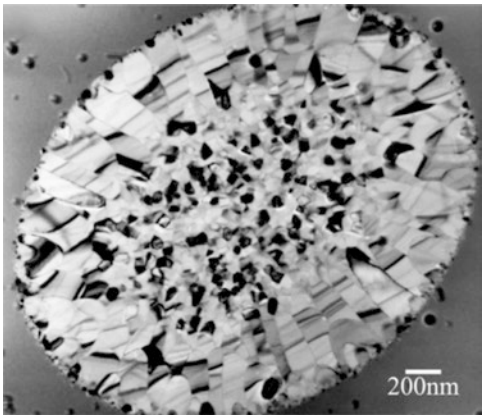

Fig. 4.7 Transmission electron micrograph of a laser-crystallized spot in an as-deposited amorphous $Ge_2Sb_2Te_5$-film. From [96]

understanding of the crystallization kinetics by developing and testing atomistic models of the phase transition.

A remarkable, now however somewhat obsolete model for Ge:Sb:Te-systems was given by Kolobov et al. [16], the so-called umbrella-flip model. It stated that the main structural rearrangement taking place upon crystallization is a flip of germanium from tetrahedral to octahedral sites. Since this model not only gave an intuitive explanation of why the phase transition proceeds so fast, yet involved a change in bonding significant enough to account for the contrast observed, it attracted much attention. The extensive theoretical simulations and experimental studies in recent years that have been addressed before, however, show that while tetrahedrally coordinated germanium-atoms are indeed present in the amorphous phase, they represent only a minority, making up only roughly one third of all germanium atoms. Also, they typically involve homopolar Ge–Ge or Ge–Sb bonds ("wrong bonds") rather than only Ge–Te bonds as stated by the umbrella-flip model.

Though a simple local structural scheme like the umbrella-flip model is appealing, it is unlikely that such a model realistically or universally accounts for the phase transition in phase-change materials. Therefore, research has shifted to molecular dynamics simulations of the amorphous phase of particular materials as discussed before, and even the simulation of complete phase-change cycles [58].

4.6 Applications Employing Phase-Change Materials

The aim of the last part of the present chapter is to give an overview over the various applications that employ phase-change materials, and an outlook on their future development.

4.6.1 Optical Storage

Presently, optical data storage devices represent the most common application of phase-change based recording. With the introduction of blue laser light and a further increase of the numerical aperture, the race for higher resolution and hence the development of this field may at first seem to have come to an end. Room for increasing storage capacity would be left only by increasing the number of data layers per disk. At present, a 100 GB disk employing three data layers marks the upper limit for such data storage devices, paving the way to the fourth generation of commercial optical phase-change based media [97]. However, another way of increasing capacity has been found in the course of phase-change research, that is near-field recording. The so-called Super-RENS effect (super-resolution near-field structure) refers to the observation that structures smaller than the diffraction limit can be fabricated by combining phase-change films with an additional thin layer in close proximity [98]. In an elegant realization, the part of the optical system that needs to be located very close to the phase-change film to enable near-field recording is incorporated into the disk structure itself. The extra layer typically functions as a dynamic aperture, which should at the same time be small and highly transmittive (aperture-type Super-RENS). Materials successfully employed for these mask layers typically comprise materials related to phase-change materials such as antimony [98, 99], Sb_2Te_3 [100] and PbTe [101] or even phase-change materials themselves [102]. The effect of super-resolution may be achieved by various types of interaction between matter and light. No consensus on the exact origin of the Super-RENS-effect using the aforementioned materials has been reached yet [102–108].

4.6.2 Electronic Storage

When phase-change materials were introduced in 1968 by Ovshinsky [1], electronic memories were among their first suggested applications. Nevertheless, only now that the discovery of fast-switching phase-change materials meets the ability to create nano-scaled structures, it is possible to create competitive, non-volatile phase-change based electronic memories: *phase-change random access memory*, usually abbreviated *PRAM* or *PCRAM*. As can be seen from the PTE-diagram shown in Fig. 4.8, operation can be facilitated on the timescale of few nanoseconds which is orders of magnitude faster than Flash. PCRAM makes extensive use of the threshold switching effect presented in Sect. 4.4.2. In order to supply sufficient Joule heating power $P_J = U \cdot I = U^2 / R(U)$ to quickly raise the temperature to levels high enough for crystallization to take place on a small timescale (cf. Fig. 4.6), very high voltages would be required, if threshold switching would not occur. Thus, it allows to avoid voltage upconversion.

Various designs of PCRAM cells have been proposed. A line-cell is simply a lateral line of a phase-change material that connects two electrodes. This concept

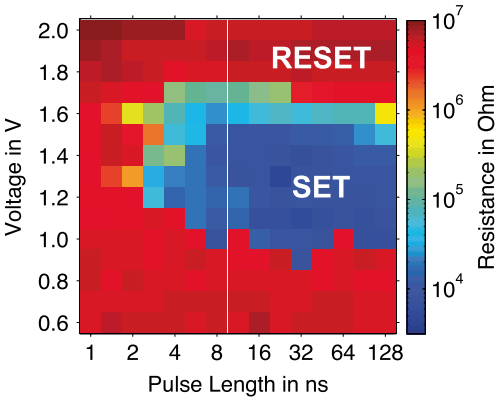

Fig. 4.8 Characterization of the re-crystallization of a PCRAM-device employing GeTe as the active material using an electric tester. The different grey scales show the resistance change upon the application of electrical pulses of given length and voltage. Crystallization can be triggered by applying pulses as short as only about 5 ns. Modified from [81]

appears advantageous due to the ease of fabrication and low power consumption of these cells [63]. More common is a vertical stack of layers, where a small volume of phase-change is located on top of a highly resistive heater element. Here, a portion of the phase-change volume that is close to the heater, that typically features a reduced diameter to increase the current density, is switched between the phases. Recently, an improved version of a PCRAM-cell has been realized that comfortably integrates the cell selector into the cell design [109]. By the use of an Ovonic threshold-switch (OTS) rather than a bipolar junction transistor, for instance, a selector with no more than the same spatial footprint as the memory cell itself (i.e., $4F^2$, F being the feature size) is possible. The OTS is just a thin layer of a material that exhibits threshold-switching. If the voltage drop over the OTS (due to the voltage applied between word- and bit-line) exceeds the threshold field, the memory cell that is in series with the OTS is selected. The simple design may also allow the stacking of layers of PCRAM-cells, increasing the storage density by making use of the third dimension.

Among the criteria for a memory technique to be promising, scalability is a key requirement. Lack of scalability is one of the reasons why alternatives to Flash memory are actively pursued. Two factors may be discerned when scalability is addressed. On the one hand, the phase-change material must retain its properties despite reduction of its volume. On the other hand, the space taken up by dielectrics and the electronics necessary to address and control the memory cell must be taken into account as well. Nano-scaling is particularly advantageous to phase-change memory, since both energy consumption and crystallization time decrease upon volume reduction. The latter stems from the fact that for small memory cells, crystallization dominantly takes place via growth. The impact of nano-scaling on the material and device characteristics has recently been summarized in a detailed report by Raoux et al. [3]. Other aspects that can be subsumed under scalability are the aforementioned prospect of stackability as well as multi-level storage via control of the amorphized volume fraction.

So far, the advantages of PCRAM over competing memory technologies have been given in terms of its non-volatility, speed, and attainable storage density.

Another aspect, however, is cyclability (i.e., the number of possible write-cycles). The two main wear processes identified so far are electromigration and void formation. It is found that for cells based on Ge:Sb:Te-materials, the spatial distribution of the elements changes upon set and reset operations. In particular, antimony accumulates at the cathode, pushing germanium aside. Thus, the composition in the active volume and thereby the cell properties change. Operation at reversed polarity, though, can "repair" such a cell [110]. The density change upon crystallization and atomic mobility may also hamper the electrical contact via void formation [111]. In addition, degradation of the electrodes (e.g., diffusion into the phase-change material) and phase segregation in the case of non-stoichiometric materials may also be regarded as limiting factors. Nevertheless, though the exact number of possible cycles depends on a variety of factors, it is generally expected to exceed the corresponding value of Flash by some orders of magnitude.

Beyond optical and electrical data storage, various further uses have been developed. To mention one notable idea, the fact that the resistivity of a phase-change cell depends on its history (i.e., more than just two logical states can be represented by one cell, multi-level storage) has led to the proposal of using such devices to emulate the behavior of synapses, paving the way for cognitive information processing [112]. In that sense, phase-change based data storage does not only hold the potential to serve as a fast and reliable, universal non-volatile memory. Moreover, this technology could also revolutionize the way we process data.

References

1. S.R. Ovshinsky, Reversible electrical switching phenomena in disordered structures. Phys. Rev. Lett. **21**(20), 1450 (1968)
2. M. Wuttig, N. Yamada, Phase-change materials for rewriteable data storage. Nat. Mater. **6**(11), 824 (2007)
3. S. Raoux, W. Welnic, D. Ielmini, Phase change materials and their application to nonvolatile memories. Chem. Rev. **110**(1), 240 (2010)
4. G.W. Burr, M.J. Breitwisch, M. Franceschini, D. Garetto, K. Gopalakrishnan, B. Jackson, B. Kurdi, C. Lam, L.A. Lastras, A. Padilla, B. Rajendran, S. Raoux, R.S. Shenoy, Phase change memory technology. J. Vac. Sci. Technol. B **28**(2), 223 (2010)
5. D. Lencer, Design rules, local structure and lattice-dynamics of phase-change materials for data storage applications, Ph.D. thesis, RWTH Aachen University (2010)
6. N. Yamada, E. Ohno, N. Akahira, K. Nishiuchi, K. Nagata, M. Takao, High-speed overwritable phase-change optical disk material. Jpn. J. Appl. Phys. **26**, 61 (1987)
7. N. Yamada, E. Ohno, K. Nishiuchi, N. Akahira, M. Takao, Rapid-phase transitions of Gete-Sb2 Te3 pseudobinary amorphous thin-films for an optical disk memory. J. Appl. Phys. **69**(5), 2849 (1991)
8. M.H.R. Lankhorst, L. van Pieterson, M. van Schijndel, B.A.J. Jacobs, J.C.N. Rijpers, Prospects of doped Sb-Te phase-change materials for high-speed recording. Jpn. J. Appl. Phys. **42**(2B), 863 (2003)
9. J. Solis, C.N. Afonso, J.F. Trull, M.C. Morilla, Fast crystallizing Gesb alloys for optical-data storage. J. Appl. Phys. **75**(12), 7788 (1994)
10. L. van Pieterson, M. van Schijndel, J.C.N. Rijpers, M. Kaiser, Te-free, Sb-based phase-change materials for high-speed rewritable optical recording. Appl. Phys. Lett. **83**(7), 1373 (2003)

11. J.L.F. Da Silva, A. Walsh, H.L. Lee, Insights into the structure of the stable and metastable (GeTe)(m)(Sb2Te3)(n) compounds. Phys. Rev. B **78**(22), 224111 (2008)
12. D. Lencer, M. Salinga, B. Grabowski, T. Hickel, J. Neugebauer, M. Wuttig, A map for phase-change materials. Nat. Mater. **7**(12), 972 (2008)
13. Z.M. Sun, J. Zhou, R. Ahuja, Structure of phase change materials for data storage. Phys. Rev. Lett. **96**(5), 055507 (2006)
14. Z. Sun, S. Kyrsta, D. Music, R. Ahuja, J.M. Schneider, Structure of the Ge-Sb-Te phase-change materials studied by theory and experiment. Solid State Commun. **143**(4–5), 240 (2007)
15. J.W. Park, S.H. Eom, H. Lee, J.L.F. Da Silva, Y.S. Kang, T.Y. Lee, Y.H. Khang, Optical properties of pseudobinary GeTe, Ge2Sb2Te5, GeSb2Te4, GeSb4Te7, and Sb2Te3 from ellipsometry and density functional theory. Phys. Rev. B **80**(11), 115209 (2009)
16. A.V. Kolobov, P. Fons, A.I. Frenkel, A.L. Ankudinov, J. Tominaga, T. Uruga, Understanding the phase-change mechanism of rewritable optical media. Nat. Mater. **3**(10), 703 (2004)
17. S. Shamoto, N. Yamada, T. Matsunaga, T. Proffen, J.W. Richardson, J.H. Chung, T. Egami, Large displacement of germanium atoms in crystalline Ge2Sb2Te5. Appl. Phys. Lett. **86**(8), 081904 (2005)
18. U.V. Waghmare, N.A. Spaldin, H.C. Kandpal, R. Seshadri, First-principles indicators of metallicity and cation off-centricity in the IV–VI rocksalt chalcogenides of divalent Ge, Sn, and Pb. Phys. Rev. B **67**(12), 125111 (2003)
19. M.C. Jung, K.H. Kim, Y.M. Lee, J.H. Eom, J. Im, Y.G. Yoon, J. Ihm, S.A. Song, H.S. Jeong, H.J. Shin, Chemical state and atomic structure of Ge2Sb2Te5 system for nonvolatile phase-change random access memory. J. Appl. Phys. **104**(7), 074911 (2008)
20. J. Akola, R.O. Jones, Density functional study of amorphous, liquid and crystalline Ge2Sb2Te5: homopolar bonds and/or AB alternation? J. Phys. Conden. Matter **20**(46), 465103 (2008)
21. S. Caravati, M. Bernasconi, T.D. Kuhne, M. Krack, M. Parrinello, First-principles study of crystalline and amorphous Ge2Sb2Te5 and the effects of stoichiometric defects. J. Phys. Conden. Matter **21**(25), 255501 (2009)
22. T. Matsunaga, H. Morita, R. Kojima, N. Yamada, K. Kifune, Y. Kubota, Y. Tabata, J.J. Kim, M. Kobata, E. Ikenaga, K. Kobayashi, Structural characteristics of GeTe-rich GeTe-Sb2Te3 pseudobinary metastable crystals. J. Appl. Phys. **103**(9), 093511 (2008)
23. M. Wuttig, D. Lusebrink, D. Wamwangi, W. Welnic, M. Gillessen, R. Dronskowski, The role of vacancies and local distortions in the design of new phase-change materials. Nat. Mater. **6**(2), 122 (2007)
24. K. Shportko, S. Kremers, M. Woda, D. Lencer, J. Robertson, M. Wuttig, Resonant bonding in crystalline phase-change materials. Nat. Mater. **7**(8), 653 (2008)
25. G. Lucovsky, R.M. White, Effects of resonance bonding on properties of crystalline and amorphous semiconductors. Phys. Rev. B **8**(2), 660 (1973)
26. P.B. Littlewood, Structure and bonding in narrow gap semiconductors. Crc Crit. Rev. Solid State Mater. Sci. **11**(3), 229 (1984)
27. A.H. Edwards, A.C. Pineda, P.A. Schultz, M.G. Martin, A.P. Thompson, H.P. Hjalmarson, C.J. Umrigar, Electronic structure of intrinsic defects in crystalline germanium telluride. Phys. Rev. B **73**(4), 045210 (2006)
28. I. Friedrich, V. Weidenhof, W. Njoroge, P. Franz, M. Wuttig, Structural transformations of Ge2Sb2Te5 films studied by electrical resistance measurements. J. Appl. Phys. **87**(9), 4130 (2000)
29. B.S. Lee, J.R. Abelson, S.G. Bishop, D.H. Kang, B.K. Cheong, Kim, K.B. Investigation of the optical and electronic properties of Ge2Sb2Te5 phase change material in its amorphous, cubic, and hexagonal phases. J. Appl. Phys. **97**(9), 093509 (2005)
30. T. Siegrist, P. Jost, H. Volker, M. Woda, P. Merkelbach, C. Schlockermann, M. Wuttig, Disorder-induced localization in crystalline phase-change materials. Nat. Mater. **10**, 202 (2010)

31. C.A. Angell, K.L. Ngai, McKenna, G.B., P.F. McMillan, S.W. Martin, Relaxation in glass-forming liquids and amorphous solids. J. Appl. Phys. **88**(6), 3113 (2000)
32. J.A. Kalb, M. Wuttig, F. Spaepen, Calorimetric measurements of structural relaxation and glass transition temperatures in sputtered films of amorphous Te alloys used for phase change recording. J. Mater. Res. **22**(3), 748 (2007)
33. J. Kalb, F. Spaepen, M. Wuttig, Calorimetric measurements of phase transformations in thin films of amorphous Te alloys used for optical data storage. J. Appl. Phys. **93**(5), 2389 (2003)
34. J.C. Phillips, Topology of covalent non-crystalline solids. 1. Short-range order in chalcogenide alloys. J. Non Cryst. Solids **34**(2), 153 (1979)
35. J.P. Gaspard, A. Pellegatti, F. Marinelli, C. Bichara, Peierls instabilities in covalent structures - I. Electronic structure, cohesion and the Z = 8-N rule. Philos. Mag. **77**(3), 727 (1998)
36. P. Boolchand, D.G. Georgiev, B. Goodman, Discovery of the intermediate phase in chalcogenide glasses. J. Optoelectron. Adv. Mater. **3**(3), 703 (2001)
37. M. Micoulaut, Linking rigidity transitions with enthalpic changes at the glass transition and fragility: insight from a simple oscillator model. J. Phys. Condens. Matter **22**, 285101 (2010)
38. M. Micoulaut, J.Y. Raty, C. Otjacques, C. Bichara, Understanding amorphous phase-change materials from the viewpoint of Maxwell rigidity. Phys. Rev. B **81**(17), 174206 (2010)
39. M.H.R. Lankhorst, Modelling glass transition temperatures of chalcogenide glasses. Applied to phase-change optical recording materials. J. Non Cryst. Solids **297**(2–3), 210 (2002)
40. J. Bicerano, S.R. Ovshinsky, Chemical-bond approach to the structures of chalcogenide glasses with reversible switching properties. J. Non Cryst. Solids **74**(1), 75 (1985)
41. S. Raoux, M. Salinga, J.L. Jordan-Sweet, A. Kellock, Effect of Al and Cu doping on the crystallization properties of the phase change materials SbTe and GeSb. J. Appl. Phys. **101**(4), 044909 (2007)
42. T. Katsuyama, H. Matsumara, Glass-forming regions of ternary Ge-Te-Al and Ge-Te-Sb chalcogenide glasses. J. Non Cryst. Solids **139**(2), 177 (1992)
43. C. Steimer, V. Coulet, W. Welnic, H. Dieker, R. Detemple, C. Bichara, B. Beuneu, J.P. Gaspard, M. Wuttig, Characteristic ordering in liquid phase-change materials. Adv. Mater. **20**(23), 4535 (2008)
44. C. Bichara, M. Johnson, J.P. Gaspard, Octahedral structure of liquid GeSb2Te4 alloy: first-principles molecular dynamics study. Phys. Rev. B **75**(6), 060201 (2007)
45. J. Akola, J. Larrucea, R.O. Jones, Polymorphism in amorphous Ge2Sb2Te5: comparison of melt-quenched and as-deposited structures, in *European Phase-Change and Ovonics Symposium 2010*, p. 128 (2010)
46. K. Hirota, K. Nagino, G. Ohbayashi, Local structure of amorphous GeTe and PdGeSbTe alloy for phase change optical recording. J. Appl. Phys. **82**(1), 65 (1997)
47. S. Hosokawa, T. Ozaki, K. Hayashi, N. Happo, M. Fujiwara, K. Horii, P. Fons, A.V. Kolobov, J. Tominaga, Existence of tetrahedral site symmetry about Ge atoms in a single-crystal film of Ge2Sb2Te5 found by x-ray fluorescence holography. Appl. Phys. Lett. **90**(13), 131913 (2007)
48. K.S. Andrikopoulos, S.N. Yannopoulos, G.A. Voyiatzis, A.V. Kolobov, M. Ribes, J. Tominaga, Raman scattering study of the a-GeTe structure and possible mechanism for the amorphous to crystal transition. J. Phys. Conden. Matter **18**(3), 965 (2006)
49. K.S. Andrikopouslos, S.N. Yannopoulos, A.V. Kolobov, P. Fons, J. Tominaga, Raman scattering study of GeTe and Ge2Sb2Te5 phase-change materials. J. Phys. Chem. Solids **68**(5–6), 1074 (2007)
50. W. Welnic, A. Pamungkas, R. Detemple, C. Steimer, S. Blugel, M. Wuttig, Unravelling the interplay of local structure and physical properties in phase-change materials. Nat. Mater. **5**(1), 56 (2006)
51. P. Jovari, I. Kaban, J. Steiner, B. Beuneu, A. Schops, A. Webb, 'Wrong bonds' in sputtered amorphous Ge2Sb2Te5. J. Phys. Conden. Matter **19**(33), 335212 (2007)
52. P. Jovari, I. Kaban, J. Steiner, B. Beuneu, A. Schops, M.A. Webb, Local order in amorphous Ge2Sb2Te5 and GeSb2Te4. Phys. Rev. B **77**(3), 035202 (2008)
53. S. Kohara, K. Kato, S. Kimura, H. Tanaka, T. Usuki, K. Suzuya, H. Tanaka, Y. Moritomo, T. Matsunaga, N. Yamada, Y. Tanaka, H. Suematsu, M. Takata, Structural basis for the fast

phase change of Ge2Sb2Te5: ring statistics analogy between the crystal and amorphous states. Appl. Phys. Lett. **89**(20), 201910 (2006)
54. J. Akola, R.O. Jones, Structural phase transitions on the nanoscale: the crucial pattern in the phase-change materials Ge2Sb2Te5 and GeTe. Phys. Rev. B **76**(23), 235201 (2007)
55. J. Akola, R.O. Jones, Binary alloys of Ge and Te: order, voids, and the eutectic composition. Phys. Rev. Lett. **100**(20), 205502 (2008)
56. J. Akola, R.O. Jones, Structure of amorphous Ge8Sb2Te11: GeTe-Sb2Te3 alloys and optical storage. Phys. Rev. B **79**(13), 134118 (2009)
57. S. Caravati, M. Bernasconi, T.D. Kuhne, M. Krack, M. Parrinello, Coexistence of tetrahedral- and octahedral-like sites in amorphous phase change materials. Appl. Phys. Lett. **91**(17), 171906 (2007)
58. J. Hegedus, S.R. Elliott, Microscopic origin of the fast crystallization ability of Ge-Sb-Te phase-change memory materials. Nat. Mater. **7**(5), 399 (2008)
59. J. Akola, R.O. Jones, S. Kohara, S. Kimura, K. Kobayashi, M. Takata, T. Matsunaga, R. Kojima, N. Yamada, Experimentally constrained density-functional calculations of the amorphous structure of the prototypical phase-change material Ge2Sb2Te5. Phys. Rev. B **80**(2), 020201 (2009)
60. M. Xu, Y.Q. Cheng, H.W. Sheng, E. Ma, Nature of atomic bonding and atomic structure in the phase-change Ge2Sb2Te5 glass. Phys. Rev. Lett. **103**(19), 195502 (2009)
61. S. Caravati, M. Bernasconi, M. Parrinello, First-principles study of liquid and amorphous Sb2Te3. Phys. Rev. B **81**(1), 014201 (2010)
62. D. Adler, M.S. Shur, M. Silver, S.R. Ovshinsky, Threshold switching in chalcogenide-glass thin-films. J. Appl. Phys. **51**(6), 3289 (1980)
63. M.H.R. Lankhorst, B.W.S.M.M. Ketelaars, R.A.M. Wolters, Low-cost and nanoscale non-volatile memory concept for future silicon chips. Nat. Mater. **4**(4), 347 (2005)
64. D. Krebs, S. Raoux, C.T. Rettner, G.W. Burr, M. Salinga, M. Wuttig, Threshold field of phase change memory materials measured using phase change bridge devices. Appl. Phys. Lett. **95**(8), 082101 (2009)
65. D. Krebs, Electrical transport and switching in phase change materials, Ph.D. thesis, RWTH Aachen University (2010)
66. D. Emin, Current-driven threshold switching of a small polaron semiconductor to a metastable conductor. Phys. Rev. B **74**(3), 035206 (2006)
67. D. Ielmini, Y.G. Zhang, Analytical model for subthreshold conduction and threshold switching in chalcogenide-based memory devices. J. Appl. Phys. **102**(5), 054517 (2007)
68. D. Ielmini, Threshold switching mechanism by high-field energy gain in the hopping transport of chalcogenide glasses. Phys. Rev. B **78**(3), 035308 (2008)
69. A. Pirovano, A.L. Lacaita, A. Benvenuti, F. Pellizzer, R. Bez, Electronic switching in phase-change memories. IEEE Trans. Electron Devices **51**(3), 452 (2004)
70. A. Redaelli, A. Pirovano, A. Benvenuti, A.L. Lacaita, Threshold switching and phase transition numerical models for phase change memory simulations. J. Appl. Phys. **103**(11), 111101 (2008)
71. K. Jandieri, O. Rubel, S.D. Baranovskii, A. Reznik, J.A. Rowlands, S.O. Kasap, Lucky-drift model for impact ionization in amorphous semiconductors. J. Mater. Sci. Mater. Electron. **20**, 221 (2009)
72. V.G. Karpov, Y.A. Kryukov, S.D. Savransky, I.V. Karpov, Nucleation switching in phase change memory. Appl. Phys. Lett. **90**(12), 123504 (2007)
73. M. Boniardi, A. Redaelli, A. Pirovano, I. Tortorelli, D. Ielmini, F. Pellizzer, A physics-based model of electrical conduction decrease with time in amorphous Ge2Sb2Te5. J. Appl. Phys. **105**(8), 084506 (2009)
74. W.K. Njoroge, H.W. Woltgens, M. Wuttig, Density changes upon crystallization of Ge2Sb2.04Te4.74 films. J. Vac. Sci. Technol. A **20**(1), 230 (2002)
75. A. Pirovano, A.L. Lacaita, F. Pellizzer, S.A. Kostylev, A. Benvenuti, R. Bez, Low-field amorphous state resistance and threshold voltage drift in chalcogenide materials. IEEE Trans. Electron Devices **51**(5), 714 (2004)

76. I.V. Karpov, M. Mitra, D. Kau, G. Spadini, Y.A. Kryukov, V.G. Karpov, Fundamental drift of parameters in chalcogenide phase change memory. J. Appl. Phys. **102**(12), 124503 (2007)
77. S. Braga, A. Cabrini, G. Torelli, Dependence of resistance drift on the amorphous cap size in phase change memory arrays. Appl. Phys. Lett. **94**(9), 092112 (2009)
78. J. Robertson, K. Xiong, P.W. Peacock, Electronic and atomic structure of Ge2Sb2Te5 phase change memory material. Thin Solid Films **515**(19), 7538 (2007)
79. D. Ielmini, D. Sharma, S. Lavizzari, A.L. Lacaita, Reliability impact of chalcogenide-structure relaxation in phase-change memory (PCM) cells-part I: experimental study. IEEE Trans. Electron Devices **56**(5), 1070 (2009)
80. B.S. Lee, G.W. Burr, R.M. Shelby, S. Raoux, C.T. Rettner, S.N. Bogle, K. Darmawikarta, S.G. Bishop, J.R. Abelson, Observation of the role of subcritical nuclei in crystallization of a glassy solid. Science **326**(5955), 980 (2009)
81. G. Bruns, P. Merkelbach, C. Schlockermann, M. Salinga, M. Wuttig, T.D. Happ, J.B. Philipp, M. Kund, Nanosecond switching in GeTe phase change memory cells. Appl. Phys. Lett. **95**(4), 043108 (2009)
82. N. Ohshima, Crystallization of germanium-antimony-tellurium amorphous thin film sandwiched between various dielectric protective films. J. Appl. Phys. **79**(11), 8357 (1996)
83. B.J. Kooi, R. Pandian, J.T.M. De Hosson, A. Pauza, In situ transmission electron microscopy study of the crystallization of fast-growth doped SbxTe alloy films. J. Mater. Res. **20**(7), 1825 (2005)
84. S. Raoux, H.Y. Cheng, J.L. Jordan-Sweet, B. Munoz, M. Hitzbleck, Influence of interfaces and doping on the crystallization temperature of Ge-Sb. Appl. Phys. Lett. **94**(18), 183114 (2009)
85. V. Weidenhof, I. Friedrich, S. Ziegler, M. Wuttig, Laser induced crystallization of amorphous Ge2Sb2Te5 films. J. Appl. Phys. **89**(6), 3168 (2001)
86. P.K. Khulbe, E.M. Wright, M. Mansuripur, Crystallization behavior of as-deposited, melt quenched, and primed amorphous states of Ge2Sb2.3Te5 films. J. Appl. Phys. **88**(7), 3926 (2000)
87. J.S. Wei, F.X. Gan, Theoretical explanation of different crystallization processes between as-deposited and melt-quenched amorphous Ge2Sb2Te5 thin films. Thin Solid Films **441**(1–2), 292 (2003)
88. M. Naito, M. Ishimaru, Y. Hirotsu, M. Takashima, Local structure analysis of Ge-Sb-Te phase change materials using high-resolution electron microscopy and nanobeam diffraction. J. Appl. Phys. **95**(12), 8130 (2004)
89. G.F. Zhou, Materials aspects in phase change optical recording. Mater. Sci. Eng. A Struct. Mater. **304**, 73 (2001)
90. B.J. Kooi, J.T.M. De Hosson, On the crystallization of thin films composed of Sb3.6Te with Ge for rewritable data storage. J. Appl. Phys. **95**(9), 4714 (2004)
91. B.J. Kooi, W.M.G. Groot, J.T.M. De Hosson, In situ transmission electron microscopy study of the crystallization of Ge2Sb2Te5. J. Appl. Phys. **95**(3), 924 (2004)
92. J. Kalb, F. Spaepen, M. Wuttig, Atomic force microscopy measurements of crystal nucleation and growth rates in thin films of amorphous Te alloys. Appl. Phys. Lett. **84**(25), 5240 (2004)
93. J.A. Kalb, F. Spaepen, M. Wuttig, Kinetics of crystal nucleation in undercooled droplets of Sb- and Te-based alloys used for phase change recording. J. Appl. Phys. **98**(5), 054910 (2005)
94. V. Weidenhof, I. Friedrich, S. Ziegler, M. Wuttig, Atomic force microscopy study of laser induced phase transitions in Ge2Sb2Te5. J. Appl. Phys. **86**(10), 5879 (1999)
95. J.A. Kalb, C.Y. Wen, F. Spaepen, H. Dieker, M. Wuttig, Crystal morphology and nucleation in thin films of amorphous Te alloys used for phase change recording. J. Appl. Phys. **98**(5), 054902 (2005)
96. I. Friedrich, V. Weidenhof, S. Lenk, M. Wuttig, Morphology and structure of laser-modified Ge2Sb2Te5 films studied by transmission electron microscopy. Thin Solid Films **389**(1–2), 239 (2001)

97. N. Yamada, R. Kojima, T. Nishihara, A. Tsuchino, Y. Tomekawa, H. Kusada, 100 GB rewritable triple-layer optical disk having Ge-Sb-Te films, in *European Phase-Change and Ovonics Symposium 2009* (2009)
98. J. Tominaga, T. Nakano, N. Atoda, An approach for recording and readout beyond the diffraction limit with an Sb thin film. Appl. Phys. Lett. **73**(15), 2078 (1998)
99. T. Fukaya, J. Tominaga, T. Nakano, N. Atoda, Optical switching property of a light-induced pinhole in antimony thin film. Appl. Phys. Lett. **75**(20), 3114 (1999)
100. L.P. Shi, T.C. Chong, X. Hu, J.M. Li, X.S. Miao, Investigation on mechanism of aperture-type super-resolution near-field optical disk. Jpn. J. Appl. Phys. **45**(2B), 1385 (2006)
101. H.S. Lee, B.K. Cheong, T.S. Lee, K.S. Lee, W.M. Kim, J.W. Lee, S.H. Cho, J.Y. Huh, Thermoelectric PbTe thin film for superresolution optical data storage. Appl. Phys. Lett. **85**(14), 2782 (2004)
102. H.S. Lee, T.S. Lee, Y. Lee, J. Kim, S. Lee, J.Y. Huh, D. Kim, B.K. Cheong, Microstructural and optical analysis of superresolution phenomena due to Ge2Sb2Te5 thin films at blue light regime. Appl. Phys. Lett. **93**(22), 221108 (2008)
103. M. Kuwahara, T. Shima, P. Fons, T. Fukaya, J. Tominaga, On a thermally induced readout mechanism in super-resolution optical disks. J. Appl. Phys. **100**(4), 043106 (2006)
104. M. Kuwahara, T. Shima, P. Fons, J. Tominaga, In-situ Raman scattering spectroscopy for a super resolution optical disk during readout. Appl. Phys. Express **2**(8), 082402 (2009)
105. J.M. Li, L.P. Shi, H.X. Yang, K.G. Lim, X.S. Miao, W.L. Tan, T.C. Chong, Local thermal expansion in super-resolution near-field structure. Jpn. J. Appl. Phys. **46**(7A), 4148 (2007)
106. J. Tominaga, T. Shima, M. Kuwahara, T. Fukaya, A. Kolobov, T. Nakano, Ferroelectric catastrophe: beyond nanometre-scale optical resolution. Nanotechnology **15**(5), 411 (2004)
107. H.S. Lee, B.K. Cheong, T.S. Lee, J.H. Jeong, S. Lee, W.M. Kim, D. Kim, Origin of nonlinear optical characteristics of crystalline Ge-Sb-Te thin films for possible superresolution effects. Jpn. J. Appl. Phys. **46**(12–16), L277 (2007)
108. J. Liu, J.S. Wei, Optical nonlinear absorption characteristics of AgInSbTe phase change thin films. J. Appl. Phys. **106**(8), 083112 (2009)
109. D. Kau, S. Tang, I. Karpov, R. Dodge, B. Klehn, J. Kalb, J. Strand, A. Diaz, N. Leung, J. Wu, S. Lee, T. Langtry, K. wei Chang, C. Papagianni, J. Lee, J. Hirst, S. Erra, E. Flores, N. Righos, H. Castro, G. Spadini, A stackable cross point Phase Change Memory, in *2009 IEEE International Electron Devices Meeting (IEDM)*, pp. 1–4 (2009)
110. S. Lee, J. hyun Jeong, T.S. Lee, W.M. Kim, B. ki Cheong, A study on the failure mechanism of a phase-change memory in write/erase cycling. IEEE Electron Device Lett. **30**(5), 448 (2009)
111. L. Krusin-Elbaum, C. Cabral Jr., K.N. Chen, M. Copel, D.W. Abraham, K.B. Reuter, S.M. Rossnagel, J. Bruley, V.R. Deline, Evidence for segregation of Te in Ge[sub 2]Sb[sub 2] Te[sub 5] films: effect on the "phase-change" stress. Appl. Phys. Lett. **90**(14), 141902 (2007)
112. S.R. Ovshinsky, Optical cognitive information processing - a new field. Jpn. J. Appl. Phys. **43**(7B), 4695 (2004)